Title

Modularity and selection of nectar traits in the evolution of the selfing syndrome in Ipomoea lacunosa (Convolvulaceae)

Journal

New Phytologist, 233(3)

ISSN

0028-646X

Authors

Liao, Irene T
Rifkin, Joanna L
Cao, Gongyuan
et al.

Publication Date

2022-02-01

DOI

10.1111/nph.17863

DR IRENE T LIAO (Orcid ID : 0000-0002-2904-4117)
DR JOANNA RIFKIN (Orcid ID : 0000-0003-1980-5557)

Article type : Regular Manuscripts

Modularity and selection of nectar traits in the evolution of the selfing syndrome in *Ipomoea lacunosa* (Convolvulaceae)

Authors: Irene T. Liao[1,2], Joanna L. Rifkin[3], Gongyuan Cao[1], Mark D. Rausher[1]
Addresses:

1) Department of Biology, Duke University, Durham, NC, 27708 USA
2) Department of Molecular, Cell, and Developmental Biology, University of California – Los Angeles, Los Angeles, CA, 90095 USA
3) Department of Ecology and Evolutionary Biology, University of Toronto, Toronto, ON, M5S 3B2, Canada

Corresponding author: Irene T. Liao, email: ireneliao@ucla.edu

Received: *11 June 2021*
Accepted: *6 November 2021*

SUMMARY

- Although the evolution of the selfing syndrome often involves reductions in floral size, pollen, and nectar, few studies of selfing syndrome divergence have examined nectar. We investigate whether nectar traits have evolved independently of other floral size traits in the selfing syndrome, whether nectar traits diverged due to drift or selection, and the extent to which quantitative trait locus (QTL) analyses predict genetic correlations.

- We use F5 recombinant inbred lines (RILs) generated from a cross between *Ipomoea cordatotriloba* and *I. lacunosa*. We calculate genetic correlations to identify evolutionary modules, test whether trait divergence was due to selection, identify QTLs, and perform correlation analyses to evaluate how well QTL properties reflect genetic correlations.

- Nectar and floral size traits form separate evolutionary modules. Selection has acted to reduce nectar traits in the selfing *I. lacunosa*. Genetic correlations predicted from QTL properties are consistent with observed genetic correlations.

- Changes in floral traits associated with the selfing syndrome reflect independent evolution of at least two evolutionary modules: nectar and floral size traits. We also demonstrate directional selection on nectar traits, which is likely independent of selection on floral size traits. Our study also supports the expected mechanistic link between QTL properties and genetic correlations.

KEY WORDS: floral modularity, genetic correlations, *Ipomoea*, nectar traits, phenotypic divergence, QTL, selection, selfing syndrome

INTRODUCTION

Phenotypic divergence often involves changes in multiple suites of characters. Characters within a suite are often developmentally or genetically integrated and form an evolutionary module, within which characters evolve in a

coordinated fashion (Wagner & Altenberg, 1996; Brandon, 1999; Armbruster *et al.*, 2014). By contrast, divergence of different modules can be more independent. In quantitative genetic terms, traits within modules evolve in a coordinated fashion because they are constrained by strong genetic correlations, whereas different modules evolve independently because genetic correlations between modules are weak (Lewontin, 1978; Lande & Arnold, 1983; Cheverud, 1984; Arnold, 1992; Brandon, 1999; Armbruster *et al.*, 2014).

The degree to which complex characters are composed of distinct evolutionary modules remains an important question in evolutionary biology. In plants, floral and vegetative traits generally constitute distinct evolutionary modules (Berg, 1960; Armbruster *et al.*, 1999; Juenger *et al.*, 2005; Ashman & Majetic, 2006; Conner *et al.*, 2014), but there is less evidence indicating whether different types of floral traits, such as flower size, nectar production, and pollen production, also constitute distinct evolutionary modules. Flowers themselves are complex structures that serve multiple functions, from attracting and rewarding pollinators to promoting efficient pollen-to-ovule transfer for reproduction (Armbruster *et al.*, 2004; Ordano *et al.*, 2008; Diggle, 2014). However, whether the formation of floral modules mirrors the differences among these functions is still unclear.

At the developmental level, unique but overlapping gene regulatory networks underlie the identity of each floral organ (*e.g.* petal, stamen, carpel, nectary) (Bowman *et al.*, 1989; Coen & Meyerowitz, 1991; Pelaz *et al.*, 2000; Chen *et al.*, 2018; Slavković *et al.*, 2021). This pattern implies that just about any number of floral evolutionary modules is possible, depending on which genes harbor the variants involved in floral evolution. If the same genes are involved in evolutionary change for all floral characters (*e.g.* genes have pleiotropic effects because they occur in multiple regulatory networks), there would be a single evolutionary module. An example would be if size changes in all floral parts involved changes in genes regulating cell size and number expressed in all cells for all floral tissues. By contrast, at least five modules (sepal, petal, stamen, pistil, nectary) would exist if only genes unique to each regulatory network are involved in evolutionary change.

Whether flowers consist of distinct evolutionary modules is of particular importance for understanding the evolution of pollination and mating system syndromes, which typically involves predictable shifts in floral size and shape and nectar and pollen production (Smith, 2016; Wessinger & Hileman, 2016). For example, the evolution the "selfing syndrome" has occurred repeatedly in angiosperms. This syndrome typically involves reductions in floral size and in nectar and pollen production, and loss of traits (e.g. scent and color) important for attracting pollinators (Barrett, 2002; Arunkumar *et al.*, 2015). This predictability could arise for either of two reasons: (1) all floral traits constitute one evolutionary module; or (2) flowers consist of distinct evolutionary modules that undergo similar patterns of selection in different lineages. Although numerous investigations have identified quantitative trait loci

(QTLs) associated with selfing-syndrome traits ((Slotte *et al.*, 2012; Sas *et al.*, 2016; Fujikura *et al.*, 2017; Wozniak *et al.*, 2020 in *Capsella*; Baldwin *et al.*, 2011; Strandh *et al.*, 2017; Frazee *et al.*, 2021 in *Collinsia*; Fenster & Ritland, 1994; Fishman *et al.*, 2002, 2015 in *Mimulus*; Duncan & Rausher, 2013b; Rifkin *et al.*, 2019b, 2021 in *Ipomoea*), few have attempted explicitly to identify floral evolutionary modules, particularly whether floral size traits and nectar traits constitute distinct modules. Only one of these studies (Rifkin *et al.*, 2021) examined nectar traits, and included only one nectar trait (nectar volume). The primary objective of this study is to distinguish between these explanations by asking whether nectar traits constitute an evolutionary module separate from other floral traits in the evolution of the selfing syndrome.

Some evidence suggests that floral size and nectar traits may not constitute distinct modules. Multiple studies have demonstrated across-species correlations between aspects of flower size and nectar production (Galetto & Bernardello, 2004; Stuurman *et al.*, 2004; Kaczorowski *et al.*, 2005; Galliot *et al.*, 2006; Katzer *et al.*, 2019). One two-part hypothesis that could explain this correlation is that (1) both nectar volume and total sugar content are proportional to nectary size; and (2) genetic changes that cause smaller flowers also produce smaller nectaries by broadly affecting the cell size or cell number for all floral tissues. If both criteria are true, nectar and floral-size traits would not constitute separate evolutionary modules. However, if either criterion is false, then nectar traits may evolve independently of floral-size traits. Because nectary size has rarely been included in studies of floral syndrome divergence (but see Stuurman *et al.*, 2004; Katzer *et al.*, 2019; Edwards *et al.*, 2021), this hypothesis has seldom been evaluated.

We ask here whether nectar and floral size traits form separate evolutionary modules in a pair of morning glory species, *Ipomoea cordatotriloba* and *I. lacunosa*, the latter of which exhibits the selfing syndrome. Our approach is to quantify divergence genetic correlations among floral traits. We use the term "divergence genetic correlations" to indicate the correlations among F2 (or later generation) individuals of genetic changes causing trait divergence between two taxa. They may differ from genetic correlations measured within one or both of the taxa because not all genes contributing to within-taxon variation have diverged between the taxa and because novel mutations not present in standing variation may have contributed to divergence. The number of floral evolutionary modules would then be reflected in the pattern of genetic correlations between traits, with a module corresponding to a set of traits that are highly correlated with each other but not with other traits (Rifkin *et al.*, 2021). Correlations among traits within a module are high because evolutionary change in those traits was due to changes in the same or similar set of genes. By contrast, traits in different modules are expected to exhibit low genetic correlations because different genes contributed to evolutionary change.

A second issue that we address is whether reduced nectar production in the selfing *I. lacunosa* was caused by selection, and if so, whether selection acted independently of any selection for reduced floral size. Comparative studies demonstrating predictable shifts in nectar characteristics (e.g. sugar composition and nectar volume) with shifts in pollinators suggest evolutionary changes in nectar are often driven by natural selection (Baker & Baker, 1983, 1990; Bruneau, 1997; Dupont *et al.*, 2004; Cronk & Ojeda, 2008). Nevertheless, a recent review revealed that only three of ten studies detected evidence for selection on nectar characteristics (Parachnowitsch *et al.*, 2019). Additionally, it is unclear whether to expect reductions in nectar traits associated with the selfing syndrome to be driven by natural selection since pollinators do not exert selection on highly selfing plants. While costs of nectar production may generate selection for trait reductions in highly selfing species, it is also plausible that trait reductions may reflect the accumulation of neutral degenerative mutations when selection exerted by pollinators is removed.

Rifkin *et al.* (2019b) demonstrated that selection was likely responsible for reduced nectar production in *I. lacunosa*, but could not determine whether this selection reflected indirect selection due to correlations with other floral traits. Here, we provide additional evidence of selection on nectar traits and ask whether that selection is independent from selection acting on floral morphological characters. A finding that nectar traits constitute a distinct evolutionary module would imply such independence.

A third issue we address is the extent to which genetic correlations can be inferred from QTL analyses, specifically whether estimates of genetic correlations from identified QTLs is similar to direct estimates of genetic correlations among traits. Many studies of floral divergence have made inferences about the genetic correlation structure of divergence based on QTL overlaps (Slotte *et al.*, 2012; Wessinger *et al.*, 2014; Kostyun *et al.*, 2019). However, these studies rarely evaluate whether correlations inferred from QTLs accurately reflect the actual genetic correlations among traits. One exception is Gardner and Latta (2007), whose analysis was restricted largely to crop species and within-species variation.

To address these three issues, we use recombinant inbred lines (RILs) from a cross between the two morning glory species to quantify divergence genetic correlations between pairs of floral size and nectar traits and identify evolutionary modules. We perform two tests to determine whether these traits have experienced divergent selection. We also perform a QTL analysis, quantify QTL overlap among traits, and estimate genetic correlations based on QTL properties. We find that nectar traits form a separate evolutionary module from floral size traits and that changes in nectar volume and sugar content are moderately influenced by nectary size. We also find additional evidence for selection on nectar traits and infer that selection to reduce nectar production was independent of

selection on floral size traits. Finally, we find that QTL properties can qualitatively, but not necessarily quantitatively, predict genetic correlations.

MATERIALS AND METHODS

Study System

Ipomoea lacunosa L. and *Ipomoea cordatotriloba* Denn. (Convolvulaceae) are sister species in series *Batatas* that likely diverged approximately 125-500 thousand years ago (Muñoz-Rodríguez *et al.*, 2018). Both are weedy species and grow widely in southeastern United States (Duncan & Rausher, 2013a; Rifkin *et al.*, 2019a; USDA, NRCS, 2021). *Ipomoea lacunosa* is highly selfing (Duncan & Rausher, 2013b), and compared to *I. cordatotriloba*, displays components of the selfing syndrome, including reductions in overall flower size, pollen amount, pigmentation, and nectar production (McDonald *et al.*, 2011; Rifkin *et al.*, 2019b; Fig. 1a).

Plant Materials

One *I. cordatotriloba* individual was crossed with one *I. lacunosa* individual to generate F1 hybrids (Duncan & Rausher, 2013b; Rifkin *et al.*, 2021). One F1 (CL5) was selfed to generate a mapping population of 500 F2s; these were selfed by single seed decent for 3 more generations to generate 322 recombinant inbred lines (RILs) at the F5 generation. Two individuals per RIL and 24-25 selfed offspring of each parent were selected for genotyping and phenotyping.

F5 Phenotyping

Prior to planting, three seed traits – length, width, and mass – were measured using calipers and a balance sensitive to 0.001 grams. Seven flower-size traits were measured on open flowers using a digital caliper ("Mitutoyo Digimatic CD6" CS): corolla width, corolla throat, corolla length, overall corolla length, sepal length, longest stamen length, pistil length (Fig. 1b). Nectar volume, nectar sugar concentration, and nectary size (Fig. 1c,d) were also quantified. For 675 out of 686 total individuals, floral and nectar traits were measured on at least three flowers per individual plant. See Supporting Information Methods S1 for a detailed explanation of how these traits were measured. Because the two parents did not differ in herkogamy (Rikfin *et al.*, 2019b, 2021), we did not include it in our study. All measured traits differ significantly between the two parent individuals (Table 1, see Results).

Genotyping and sequencing data

Most phenotyped individuals were also genotyped (Table S1). DNA was extracted using the GeneJET ThermoFisher Plant Genomic DNA Purification Kit (Thermo Fisher Scientific). We used a modified double-digest restriction assisted DNA (ddRAD) library preparation protocol (Peterson *et al.*, 2012) combined with the Rieseberg lab genotype-by-sequencing protocol (Ostevik, 2016; Methods S2). All samples were pooled in equal amounts (100 ng) before sequencing over 4 lanes of the Illumina HiSeq 4000 platform (150bp PE reads) at the Duke Center for Genomic and Computational Biology Sequencing and Genomic Technologies Core. Raw sequence data are deposited in the NCBI Sequence Read Archive [accession: PRJNA732507].

Sequence processing and genetic map

Markers determined from ddRAD sequencing reads were aligned to the draft *I. lacunosa* genome using NextGenMap (Sedlazeck *et al.*, 2013), and a linkage map for F5 individuals was constructed concurrently with F2 individuals (Rifkin *et al.*, 2021) using Lep-Map3 (Rastas, 2017; Methods S3). This process resulted in a total of 6056 markers with 174-625 markers per linkage group (Fig. S1). A "consensus" genotype was found at each position for each RIL by comparing the genotypes between the two individuals; if the genotypes were the same, the genotype was kept. All other scenarios were coded as missing data. Overall, there was 11% missing genotype data.

Summary statistics

The final dataset includes 635 phenotyped individuals: 313 RILs with both replicates phenotyped; 9 RILs with only one individual phenotyped. Of the 635 individuals, at least three flowers were measured on 624, with the remaining 11 individuals having only one or two flowers measured. Summary statistics were calculated in R version 4.0.2 (R Core Team, 2020).

Correlations & heritabilities

Genetic correlations were calculated for all traits on F5 RILs in two ways: (1) as the correlation of line means, and (2) from variance and covariance components in a Multivariate Analysis of Variance, in which line is the main effect (Falconer & Mackay, 1996; Methods S4). Because the variance and covariance based genetic correlations are calculated from inbred lines, they represent "broad-sense" genetic correlations (Milligan *et al.*, 2003) where the variance and covariance components represent total, rather than additive, genetic variation. A broad-sense genetic correlation is thus analogous to a broad-sense heritability, which is the proportion of phenotypic variance due to total, rather than additive, genetic variance. Broad-sense heritabilities were calculated for each trait in a similar fashion (Methods S4).

Cluster analysis

We used cluster analysis to identify evolutionary modules using three algorithms: Complete, Ward, and McQuitty with the function *hclust* (Müllner, 2013) in R. All gave similar results (Fig. S2). We computed the average and standard error of pairwise trait genetic correlations within and between each module. As an indication of whether the identified modules are real, we performed a permutation test (Methods S5).

QTL analysis

QTL analyses were performed using both *qtl* (Broman *et al.*, 2003) and *qtl2* (Broman *et al.*, 2019) with the consensus genotypes and the average phenotypic values for each RIL. Most traits were approximately normally distributed, except for seed mass, seed width, nectar volume, and nectary size, which have slightly skewed distributions (Fig. S3).

We first used *qtl2* to identify QTLs using the scan1 function with a linear mixed model leave-one-chromosome-out (LOCO) method (Yang *et al.*, 2014; Broman *et al.*, 2019) with genome-wide LOD significance thresholds (α= 0.05, 1,000 permutations) and chromosome-wide LOD significance thresholds (α= 0.05, 10,000 permutations). We then used a multiple QTL mapping approach in *qtl* with the Haley-Knott regression method to determine non-spurious QTLs using the scantwo function to determine the penalties at α=0.05 to use in the stepwiseqtl function. We started the multiple QTL model selection with genome-wide significant QTLs identified with the LOCO method, searching for only for additive QTLs. Confidence intervals were estimated at 1.5-LOD intervals.

We created two QTL datasets from these approaches. The first (designated "GWS QTLs") combined the QTLs significant genome-wide from the LOCO method and from the multiple QTL model. The second dataset ("ALL QTLs") included all QTLs significant at the chromosome-wide thresholds, including multiple QTL peaks within a chromosome and most GWS QTLs, from the LOCO method.

We calculated the relative homozygous effect (RHE) as the difference between the mean trait values of homozygotes at the trait QTL peak divided by the difference between the mean trait values of the two original parents. RHE is positive (negative) if the direction of the effect is in the same (opposite) direction as the difference between parents. Summing the RHE values for a trait provides an indication of the completeness of QTL discovery: A value substantially less than 1.0 indicates that a substantial number of QTLs have not been detected, whereas a value near 1.0 suggests most QTLs affecting a trait have been identified.

Downstream analyses were performed separately for both the GWS QTLs and ALL QTLs datasets. Because the latter provides at least as good an explanation for predicted genetic correlations, we focus our analysis on the ALL QTLs dataset. Results for GWS QTLs are found in Notes S1.

Predicting genetic correlations from QTL properties

Genetic correlations include the effects of all QTLs, detected and not detected, that influences a trait. Using properties of detected QTLs to infer genetic correlations is likely to be less reliable because typically not all QTLs affecting a trait are identified in QTL studies. To determine how well the genetic correlations among traits are predicted by QTL properties, we examined properties of QTL co-localization. We considered QTLs for two traits to co-localize if their 1.5-LOD confidence intervals overlapped (Slotte *et al.*, 2012; Wessinger *et al.*, 2014; Kostyun *et al.*, 2019). To determine whether the overall degree of overlap was greater than expected by chance, we performed a randomization test (Methods S6). We quantified the degree of QTL overlap between two traits, examined whether QTL overlap could explain the observed modularity, and determined whether there was greater overlap within modules than between modules using a permutation test. We also assessed how well QTL overlap explained the observed genetic correlations (Methods S7).

We calculated a "predicted" genetic correlation from QTL properties, r_Q, using a modification of the approach presented in Gardner and Latta (2007) (Methods S8). We assessed how well r_Q matched the estimated true genetic correlations (r_G) by the correlation between r_Q and r_G. We also calculated the correlation between average total RHE for a trait pair and genetic correlation estimation bias, which is the difference between the predicted and observed genetic correlations ($r_Q - r_G$) (Gardner & Latta, 2007). To determine the significance of these correlations, we performed a permutation analysis (Methods S8). Finally, we determined whether bias involving floral and nectar traits differed for the two QTL sets by bootstrapping (1,000 replicates).

Analyses of selection

To test for whether selection contributed to the divergence of the 13 traits, we used the *v* test from Fraser, 2020 (Methods S9) and the QTL-EE sign test (Orr, 1998). Because the QTL-EE test cannot detect selection if there are fewer than eight QTLs for a trait, we applied this test only to traits with eight or more QTLs. Additionally, we performed simulations to evaluate the extent to which ascertainment bias might contribute to an increased false discovery rate (Notes S2, Anderson & Slatkin, 2003).

RESULTS

Phenotypic differences

All traits differed significantly between the parental individuals ($P < 0.05$ for all traits after correction for false discovery rate (Benjamini & Hochberg, 1995; Table 1)), consistent with our previous study. Of the traits not examined previously, nectary size was smaller, and seed mass, seed width, and seed length were larger in the *I. lacunosa*.

Nectar traits

Nectar volume (NV) and total sugar amount (TS) are highly correlated ($r = 0.98$; Fig. S4b,c). Both traits also exhibit strong and significantly non-linear relationships with nectary size, (R^2 values~0.92), indicating that the regressions account for much of the variation seen in nectar volume and total sugar amount (Fig. S4d,e). The predicted relationship between sugar concentration (NSC) and nectary size (NS), NSC(NS) = TS(NS)/NV(NS), is very similar to the observed relationship (Fig. S4f). Because total sugar amount is a derived value with a nearly exact correspondence with nectar volume, we do not include total sugar amount in subsequent analyses.

Table 1 Summary of means and standard errors of 13 traits.

Category	Trait	Units	*Ipomoea cordatotriloba*	F5 hybrids	*Ipomoea lacunosa*
Seed	Seed Length*	mm	4.194 (0.0378)	4.416 (0.0182)	4.621 (0.036)
Seed	Seed Mass*	g	0.0242 (0.000678)	0.0285 (0.000236)	0.0292 (0.000555)
Seed	Seed Width*	mm	3.836 (0.0383)	4.016 (0.0142)	4.156 (0.0322)
Nectar	Nectar Sugar Concentration	mg/mL	382.845 (2.729)	311.498 (1.75)	247.743 (6.474)
Nectar	Nectar Volume	µl	3.239 (0.131)	1.55 (0.0301)	0.517 (0.0445)
Nectar	Nectary Size	mm3	0.186 (0.0077)	0.102 (0.0016)	0.058 (0.00251)
Flower size	Sepal Length	mm	11.539 (0.0965)	11.085 (0.0432)	10.876 (0.137)
Flower size	Corolla Width	mm	28.101 (0.288)	21.858 (0.107)	16.424 (0.263)
Flower size	Corolla Throat	mm	7.446 (0.0769)	6.509 (0.0267)	5.588 (0.0667)
Flower size	Pistil Length	mm	16.025 (0.163)	13.945 (0.0758)	10.748 (0.145)
Flower size	Longest Stamen Length	mm	19.418 (0.111)	15.954 (0.0653)	12.467 (0.114)
Flower size	Corolla Length	mm	26.606 (0.198)	22.566 (0.0906)	17.526 (0.214)
Flower size	Overall Corolla Length	mm	32.357 (0.244)	26.573 (0.106)	20.066 (0.277)

Means and standard errors were calculated for *Ipomoea cordatotriloba* (n=25; 24 selfed offspring, 1 parent) and *I. lacunosa* (n=26; 25 selfed offspring, 1 parent) and F5 RILs (F5, n = 322). All traits are significantly different ($P < 0.05$) from a t-test and corrected for multiple hypotheses testing (Benjamini & Hochberg, 1995). Asterisks indicate the traits (all seeds) that do not include the parents in the mean and standard error calculations.

Genetic correlations and evolutionary modules

Genetic correlations calculated from the variance-covariance components are similar to those calculated from the RIL means ($r = 0.981$, $p < 0.05$, Fig. S5). We thus used only the former in subsequent analyses.

All traits have substantial broad-sense heritabilities (0.400-0.724). Nectar traits have lower heritabilities (0.4-0.565), and seed traits have higher heritabilities (0.62-0.724; Table S2).

Pairwise genetic correlations are positive for all traits (Table S3, Fig. S6b,c). The three clustering algorithms produced similar results: The 13 traits form three distinct clusters, which we interpret as evolutionary modules. The "flower module" consists of all floral size traits, the "nectar module" consists of the three nectar traits, and the "seed module" consists of the three seed-size traits (Fig. 2, S2). The average of correlations within modules (mean across modules = 0.602) is more than 5 times higher than the average of correlations between traits in different modules (mean = 0.117; Table 2a). A permutation test that randomly assigned the observed correlations to trait pairs indicated that the modules identified reflect groups with correlations that are higher than expected by chance. In 1,000 permutations, no values of the difference between average correlations within and between modules was as large as the observed difference of 0.485, allowing rejection of the null hypothesis at $P < 0.001$. Generally, this pattern suggests that evolution of the three modules has been largely genetically independent. Nevertheless, a moderate average genetic correlation (0.226) exists between floral and nectar traits (Table 2a), suggesting that there may have been some correlated evolution of these two modules.

QTL analyses: number and effect sizes

We detected a total of 146 QTLs (92 genome-wide significant and 54 CWS; Fig. 3, S7, Table S4). QTLs were located throughout the genome with 4-17 QTLs per chromosome. Most traits have more than five QTLs detected, except for seed mass and seed width. Most QTLs are of small (RHE less than 0.1) to moderate (RHE between 0.1-0.5) effect (Table S4, S5). All traits had a mean RHE less than 0.15 in absolute value, nine traits had a maximum RHE less than 0.25, and seed traits had a maximum RHE less than 0.5. For floral traits, total RHE values are relatively high (0.721 – 1.562, mean = 1.013), suggesting that the identified QTLs account for much of the

difference between the two species (Table S5b). Less is accounted for by nectar traits (0.563 – 0.904, mean = 0.740), indicating the existence of an unknown number of undetected QTLs. Finally, we were least successful in recovering QTLs for seed traits (-0.008 ─ -0.987, mean = - 0.416).

Table 2 Average genetic correlations and QTL overlap within and between modules.

a) GENETIC CORRELATIONS

MODULE	seed	nectar	flower
seed	0.651 (0.0655)	0.117 (0.0224)	0.0077 (0.0087)
nectar	0.117 (0.0224)	0.557 (0.1189)	0.226 (0.0177)
flower	0.0077 (0.0087)	0.226 (0.0177)	0.601 (0.0381)

b) QTL OVERLAP

MODULE	seed	nectar	flower
seed	0.460 (0.111)	0.216 (0.049)	0.214 (0.031)
nectar	0.216 (0.049)	0.500 (0.096)	0.360 (0.024)
flower	0.214 (0.031)	0.360 (0.024)	0.459 (0.028)

a) Average genetic correlations calculated from variance and covariance components. Average within- and between-module correlations are 0.602 and 0.117, respectively. Permutation test of hypothesis that within-module correlations do not differ from between-module correlations: $P < 0.001$. b) Average QTL overlap. Average within- and between-module correlations are 0.464 and 0.275, respectively. Permutation test of hypothesis that within-module correlations do not differ from between-module correlations: $P = 0.047$.

QTL overlap and genetic correlations

The pattern of average QTL overlap is similar to that exhibited by genetic correlations (Tables 2, S6). The average within-module QTL overlap was greater than that between modules (Table 2b). The within-module overlap averages are more similar to the corresponding genetic correlation averages, while the between-module averages are somewhat higher (Table 2). The within- and between-module averages of the predicted genetic correlations, r_Q, also show similar patterns when compared to the observed genetic correlations (Tables 2, S7).

The randomization test, in which we assigned each QTL to a random position in the genome and calculated the resulting QTL overlap (Table S8), indicated that there is greater overlap among QTLs within modules than would be expected by chance, consistent with within-module pleiotropy of QTLs. The test is significant both over all the modules combined and for each module individually (Table S8b).

For individual trait pairs, rather than the module averages considered above, QTL overlap and the predicted genetic correlations, r_Q, are qualitatively reflective of the magnitude of the corresponding genetic correlations, r_G. The correlation between r_G and the QTL overlap is significant (Fig. 4), as is the correlation between r_G and r_Q (Fig. 5a, Table S9). A subset of r_Q values is negative and correspond largely to pairwise correlations that include at least one seed trait. Omitting seed traits, the correlation between r_G and r_Q is reduced somewhat but remains highly significant (Figs. 5b, S8). These patterns suggest that the magnitude of QTL overlap and the predicted genetic correlations qualitatively capture the observed genetic correlations between traits reasonably well.

Analysis of selection

A strong preponderance of QTLs with RHE in the direction of the species difference ("consistent-directional QTLs") compared to the opposite direction ("contra-directional QTLs") is an expected signature of selection. Overall, 81.5% of QTLs were consistent-directional (Table S10), a pattern consistent with selection acting on many of the traits examined.

Both the QTL-EE sign test and the Fraser test support this inference. With the former test, all floral size and nectar traits, except for sepal length, were found to be nominally significant, with most remaining significant after correcting for multiple comparisons (Table S4B). The Fraser *v* test statistic is highly significant for all traits (all $P < 0.002$ nominally, $P < 0.01$ after sequential Bonferroni correction; Table 3), except sepal length and all three seed traits. Overall, these results are consistent with selection having acted on all three nectar traits and all floral traits except sepal length, and agree with findings from a previous QstFst analysis (Rifkin *et al.*, 2019b).

Contra-directional QTLs weaken the ability to detect selection because the alleles fixed are assumed to be due to genetic drift. However, another possibility is that contra-directional QTLs may have advantageous pleiotropic effects on other characters (or are tightly linked with QTLs for other characters) and were fixed because of those positive effects. This possibility could be rejected if few contra-directional QTLs overlapped consistent-directional QTLs. However, most floral size and nectar contra-directional QTLs overlap with at least one other floral or nectar QTL with consistent-directional effects (Tables S11, S12). Thus, our results are consistent with this hypothesis, but

do not prove it definitively. If true, however, it would suggest that the role of selection in the evolution of these traits is even stronger than is revealed by the Fraser and QTL-EE sign tests.

Anderson and Slatkin (2003) demonstrate that ascertainment bias can increase the rate of false positives in the QTL-EE test and likely also for the Fraser test. However, their analyses implemented an extreme version of ascertainment bias, in which the most diverged trait was chosen out of N candidate traits measured. Because this likely does not reflect how organismal traits are selected for analysis (see Notes S2), we performed simulations that relax this assumption (Notes S2). Briefly, we assume that traits for study are chosen randomly from the βN candidate loci with the highest divergence. β is thus an index of

Table 3 Fraser (2020) test for selection on each trait.

	Between-Species Variance Component	Number of CORD parents	CORD parent variance	Number LAC parents	LAC parent variance	F5 Between-Line variance component	F5 Within-Line variance component	F5 Phenotypic Variance	*v* (test statistic)	P (significance of test)
Corolla Width	66.656	25	1.759	26	1.801	2.450	2.261	4.678	27.339	0.00001526*
Corolla Throat	1.687	25	0.146	26	0.116	0.155	0.137	0.290	10.895	0.001*
Corolla Length	41.030	25	1.016	26	1.186	1.652	1.849	3.489	24.867	1.5259E-05*
Overall Corolla Length	74.652	25	1.434	26	1.993	2.515	2.094	4.583	29.795	1.5259E-05*
Sepal Length	0.203	25	0.243	26	0.490	0.363	0.446	0.806	0.482	0.490
Longest Stamen Length	23.796	25	0.255	26	0.337	0.911	0.801	1.692	26.400	1.5259E-05*
Pistil Length	13.970	25	0.686	26	0.545	1.480	0.702	2.173	9.443	0.002
Seed Mass	0.000	24	0.000	25	0.000	0.000	0.000	0.000	0.874	0.350
Seed Length	0.090	24	0.034	25	0.033	0.088	0.034	0.121	0.989	0.320
Seed Width	0.050	24	0.035	25	0.026	0.048	0.034	0.081	0.992	0.320
Nectar Volume	3.557	25	0.374	26	0.052	0.161	0.242	0.402	22.016	1.5259E-05*
Nectar Sugar Concentration	9056.500	25	191.533	26	1089.830	602.835	714.065	1312.340	14.993	0.0001*
Nectary Size	0.008	25	0.001	26	0.000	0.001	0.000	0.001	12.788	0.0004*

Columns are components of Equation [2] in Fraser (2020) with broad-sense heritabilities found in Supporting Information Table S2, *v* statistic given by that equation, and probability of *v* being as large or larger than observed by chance. A *c* value of 1.0 was used in all calculations (Methods S9). All significant P values remain significant at an overall level of $P < 0.01$ after a sequential Bonferroni correction for multiple comparisons (indicated by asterisks). CORD = *Ipomoea cordatotriloba*. LAC = *Ipomoea lacunosa*.

the intensity of ascertainment bias, with low values indicating high intensity. In Anderson and Slatkin's study, $\beta = 1/N$. We find that to correct for ascertainment bias, the probability value from the test must be multiplied by β to obtain the true probability. Although there is no theoretical or empirical guidance, it is unrealistic to assume that traits chosen for study are among the top 0.15 or less (see Notes S2 for justification). Thus, we interpret a P value of less than $0.05 \bullet 0.15 = 0.0075$ as strong evidence for selection despite any ascertainment bias. It may even be unlikely to choose traits from among the top 0.4 most diverged traits, which would mean that a P value of less than $0.05 \bullet 0.4 = 0.02$ may be consistent with selection. Based on these criteria, our analyses indicate that, except for corolla throat and pistil length, the signatures of selection we detected on floral size and nectar traits are not likely an artifact of such bias (Notes S2).

DISCUSSION

Nectar Traits and Floral Size Traits are Separate Evolutionary Modules

Flowers are complex structures that perform a variety of functions that are affected by floral size and shape, nectar production, and pollen production. Divergence in these traits is common between closely related species due to changes in either the predominant pollinators or favored mating system. Whether this divergence is constrained by pleiotropy and genetic correlations among floral traits is a long-standing question in plant evolutionary biology (Smith, 2016; Wessinger & Hileman, 2016; Kostyun *et al.*, 2019). While some recent studies have attempted to identify the degree of genetic correlations and modularity among floral traits among species (Dellinger *et al.*, 2019; Dellinger, 2020; Reich *et al.*, 2020), we are still largely ignorant of whether flowers consist of distinct evolutionary modules and, if so, what those modules are.

The flowers of *Ipomoea lacunosa* and *I. cordatotriloba* consist of at least two distinct evolutionary modules: floral size traits and nectar traits. A previous study of these species only examined one nectar trait (nectar volume), which clustered with floral size traits (Rifkin *et al.*, 2021). By including additional nectar traits, we could distinguish these modules by the moderately high within-module genetic correlations, but low between-module correlations (Table 2a). This pattern is also reflected in the degree of QTL overlap, which is on average higher within the two modules than between them. These results indicate that the evolution of decreased floral size in *I. lacunosa* has been largely genetically independent of the evolution of reduced nectar production and *vice versa*.

Evolutionary modularity can be interpreted as the independence of developmental modules (Wagner & Altenberg, 1996; von Dassow & Munro, 1999; Wagner *et al.*, 2007; Klingenberg, 2008). Often, developmental modules are

conceived of as gene regulatory networks (GRNs) (*e.g.* Melo *et al.*, 2016; Verd *et al.*, 2019; Lewis & Van Belleghem, 2020), with independence of two modules inversely related to the number of genes shared between their two GRNs. Although little is known about the GRNs associated with nectar production and nectary development, the low to moderate QTL between floral and nectar traits suggests there may be low overlap between the GRN(s) of these modules. It is also possible that there is substantial overlap of the GRNs, but most variants identified for each group are in genes that are unique to each GRN. Distinguishing between these and other developmental explanations for the distinctness of the floral size and nectar evolutionary modules in *I. lacunosa* must await detailed genetic dissection of the GRNs underlying the development of all floral parts, including the nectary.

One possibility for the independence of floral size and nectar modules is a difference in the developmental timing of these traits. Although the development of the flower and the floral nectary are undoubtedly linked, they may differ in the timing of cell fate specification and the coordination between cell division and expansion. The nectary often develops *after* floral organs have been specified (Smyth *et al.*, 1990; Baum *et al.*, 2001; Thornburg, 2007; Jeiter *et al.*, 2017); in these *Ipomoea* species, the nectary is not visibly present in the earliest stages of flower development when the four major floral organs are easily identifiable (personal observation).

Limited information exists in other species regarding the genetic and evolutionary independence of floral size and nectar traits. Across multiple species within the same genus, floral size is phylogenetically correlated with nectar volume (Galetto & Bernardello, 2004; Kaczorowski *et al.*, 2005; Tavares *et al.*, 2016), but such patterns are uninformative about evolutionary independence. Within species, artificial selection for floral size in *Eichhornia paniculata* resulted in a correlated response in nectar volume, indicating that size and nectar volume are genetically correlated, but the magnitude of the correlation is unknown (Worley & Barrett, 2000). Genetic correlations between aspects of flower size and nectar production in *Nicotiana alata* were non-significant (Kaczorowski *et al.*, 2008), consistent with the existence of separate floral size and nectar modules. However, the genetic correlations of within-species variation is not necessarily indicative of the divergence genetic correlations for two reasons: (1) genetic correlations can change under selection (Sheridan & Barker, 1974; Mitchell-Olds & Rutledge, 1986; Falconer & Mackay, 1996; Roff, 2007; Arnold *et al.*, 2008), and (2) new mutations do not necessarily reflect the correlation structure of standing genetic variation.

A few QTL studies have examined nectar trait divergence between species that have transitioned between pollinator types, but most report only divergence phenotypic correlations between aspects of floral size and only one or two nectar traits (Galliot *et al.*, 2006; Nakazato *et al.*, 2013; Katzer *et al.*, 2019; Edwards *et al.*, 2021). These studies reveal moderate to complete QTL overlap (range 0.4 –1.0) and moderate to high divergence phenotypic

correlations (0.53 – 0.742) between floral size and nectar traits (Table S13). These findings are not completely in line our results, perhaps because the processes underlying transitions in primary pollinators likely differs from transitions in mating system. Transitions from bee to hummingbird pollination often result in high nectar volume and low sugar concentration, while transitions to selfing results in reductions in nectar volume and sugar concentration. Thus, the divergence correlation structure in these species pairs may differ substantially from that we report. If so, it would suggest either that the composition and overlap of GRNs controlling floral size and nectar traits differ among species, or that genes causing divergence in these characters differ between species in the proportions that are common to both networks.

Structure of the Nectar Module

Galetto and Bernadello (2004) report a correlation between nectar volume and nectary size across six *Ipomoea* species. Additionally, within *Nicotiana alata*, there is a high genetic correlation (0.89) between nectar volume and nectar energy content (total sugar amount) (Kaczorowski *et al.*, 2008). These two findings suggest that, physiologically, nectar volume and sugar content are proportional to nectary size. If the hypothesis is true, evolutionary changes in nectar volume and sugar content could primarily be correlated responses to changes in nectary size. Although this hypothesis is not supported in the divergence for *Petunia axillaris* and *P. integrifolia*, where nectar volume and nectar sugar concentration differ between the two species but the nectary size remains the same (Stuurman *et al.*, 2004), it may be true for other species, such as *Aquilegia brevistyla* and *A. canadensis* (Edwards *et al.*, 2021).

Our results are somewhat consistent with this hypothesis. Nectar volume and total sugar content are each moderately genetically correlated with nectary size (0.70 and 0.76, respectively, Fig. S4c) and highly correlated with each other (Fig. S4b,c). Sugar concentration is also positively genetically correlated with nectary size ($r \approx 0.646$), and both nectar volume and nectar sugar concentration have moderately high QTL overlap with nectary size (0.66 and 0.5, respectively, Table S5). However, with genetic correlations of this magnitude, correlated responses to selection on nectary size would explain less than half of the variation in nectar volume and total sugar. The rest would be accounted for by mutations that affect volume and/or total sugar but not nectary size. Even within the nectar module, there is substantial independent evolution of the component traits.

Selection on Floral Size and Nectar Traits

Whether selection or drift has contributed to trait reductions in the selfing syndrome remains an outstanding question. Because floral displays and rewards are no longer necessary to attract pollinators for successful reproduction, selection may favor reductions in these potentially costly traits and reallocate resources to other

functions (Goodwillie *et al.*, 2010; Duncan & Rausher, 2013b; Rifkin *et al.*, 2019b). Drift is also plausible given that selfing plants may no longer experience purifying selection to maintain large floral displays and rewards, allowing neutral degenerative mutations to accumulate.

Two QstFst studies determined that natural selection contributed to the divergence of five floral size and two nectar traits between *Ipomoea lacunosa* and *I. cordatotriloba* (Duncan & Rausher, 2013b; Rifkin *et al.*, 2019b). However, neither study was able to distinguish between selection acting directly on these characters and indirect selection due to correlations with other selected characters. The QTL-EE sign test and the Fraser test presented here also reveal that divergent selection likely operated on both floral size and nectar traits. By combining these results with our information that floral size and nectar traits form separate evolutionary modules, we infer that selection to reduce some nectar traits occurred independently from selection on some floral size traits. However, because of the high within-module genetic correlations, we cannot distinguish direct and indirect selection on traits within the same module. Moreover, we cannot rule out the possibility that selection on the measured nectar traits is indirect, primarily due to correlations of nectar traits with other unmeasured (possibly non-nectar) traits.

Ascertainment biases, in the form of choosing to study characters that are known to have diverged between species, can bias both QTL-EE sign tests and the Fraser test, artificially increasing the probability of obtaining false positives (Anderson & Slatkin, 2003). However, ascertainment biases likely do not account for the apparent selection on nectar and floral size traits for three reasons. First, our results are consistent with previous selection detected by a completely different method (Duncan & Rausher, 2013b; Rifkin *et al.*, 2019b). Second, nine of ten floral size and nectar traits are highly significant ($P < 0.002$) by the Fraser test (Table 3), and for seven of these traits, neutrality can be rejected if they were chosen for study from more than the top 15% of candidate traits in terms of divergence (Notes S2). Finally, for these seven traits, the maximum number of candidate traits from which each of those traits can be drawn for rejection of neutrality is likely much higher than the actual number of candidate traits. Generally, the results of our analyses of ascertainment bias also indicates that they likely do not inflate the probability of false positives nearly as much as suggested by Anderson and Slatkin.

Do Identified QTLs Predict the Genetic Correlation Structure of Divergence?

QTL studies often infer the direction and magnitude of constraints on evolution, as embodied in genetic correlations, from patterns of QTL overlap (*e.g.* Slotte *et al.*, 2012; Wessinger *et al.*, 2014; Kostyun *et al.*, 2019). Seldom, however, is the validity of these inferences evaluated by comparing the patterns of QTL overlap and the actual genetic correlations among traits. One exception is a meta-study by Gardner and Latta (2007), which used QTL properties from published studies to predict genetic correlations among traits and compared those estimates

to actual genetic correlations. Because most of the studies examined quantified patterns of within-species variation, it is unclear whether these patterns can be extended to the genetic architecture of divergence between species.

Our results indicate that QTL properties can predict the qualitative pattern of genetic correlations reasonably well. The magnitudes of the observed genetic correlations are positively correlated with QTL overlap and with predicted genetic correlations, with the strength of the correlation being similar to or higher than reported by Gardner and Latta (Fig. 5a,b). This conclusion also extends to the modular nature of divergence: The average QTL overlap within and between modules generally mirrors the average genetic correlations within and between modules. More specifically, trait pairs with high genetic correlations have relatively high QTL overlap because a higher proportion of QTLs affecting these trait pairs are overlapping and presumably pleiotropic (Fig. 4).

By contrast, quantitative predictions of genetic correlations showed significant bias. In general, the magnitude of the predicted correlations was less than that of the observed correlations (Fig. 5c,d). This bias was small for floral size and nectar traits but was substantial for trait pairs that included at least one seed trait. In the latter case, the sign of the predicted correlation was generally opposite that of the observed correlations. These biases may reflect unidentified QTL that have a different overall effect on the genetic correlations than the identified QTLs, as supported by the relationship between total RHE and bias. RHE can be interpreted as an index of the completeness of QTL identification despite the tendency for QTL effects to be overestimated in studies with fewer than 500 individuals (Beavis *et al.*, 1994; Xu, 2003). Our results indicate that the bias of the predicted genetic correlations is inversely proportional to the degree to which all QTLs affecting the traits have been identified. Total RHE was generally high for flower size and nectar traits, and the corresponding genetic correlations had only a small bias. By contrast, total RHE was low for seed traits, and the bias in the predicted correlation was substantial. We conclude that one should be cautious when making inferences about genetic correlation structure and constraints on evolution based on QTL overlap unless there is evidence that most of the QTLs affecting the traits of interest have been identified.

ACKNOWLEDGEMENTS

We would like to thank members of the Rausher lab for feedback and advice on the experimental design, analyses, and manuscript; and Fred Nijhout for use of the lab's microscope and camera for imaging nectaries. We would particularly like to thank Wendy Dong, Melissa Baldino, Avery Fulford, and Cristian Tolento and members of the Duke Greenhouse Staff, who all helped with plant care and maintenance. Finally, we would like to thank three

anonymous reviewers for improving the manuscript. This research was supported in part by NSF grant DEB 1542387.

AUTHOR CONTRIBUTIONS

ITL and MDR designed the project, collected and analyzed the data, and wrote the manuscript. JLR performed final computational analyses for the linkage map and edited the manuscript. GC annotated the draft genome necessary for the randomization test.

DATA AVAILABILITY

Raw sequence data from this study are found NCBI Sequence Read Archive [accession: PRJNA732507]. Scripts for sequence processing and linkage mapping are openly available on GitHub at https://github.com/joannarifkin/Ipomoea_QTL/. All other scripts and data are openly available on GitHub at https://github.com/itliao/IpomoeaNectarQTL.

ORCID

Irene T. Liao: orcid.org/0000-0002-2904-4117
Joanna L. Rifkin: orcid.org/0000-0003-1980-5557
Gongyuan Cao: orcid.org/0000-0003-4417-251X
Mark D. Rausher: orcid.org/0000-0002-6541-9641

SUPPORTING INFORMATION

Fig. S1 Genetic map and distribution of the 6056 markers used for the QTL analysis.
Fig. S2 Cluster diagrams based on covariance-component genetic correlations.
Fig. S3 Frequency distributions of 14 phenotypic traits.
Fig. S4 Pairwise correlations and regressions for the three measured nectar traits and total sugar content.
Fig. S5 Comparison of correlations derived from RIL means and from variance-covariance (var-covar) components
Fig. S6 Pairwise trait correlations among the 13 traits.
Fig. S7 QTL plots for individual traits.
Fig. S8 Scatterplot comparison of genetic variances and covariances derived from RIL phenotypes and QTL properties.

Methods S1 Materials and growing conditions and phenotyping nectar traits (nectar volume, nectar sugar concentration, nectary size).
Methods S2 Summary protocol for ddRAD sequencing.
Methods S3 Sequence processing and linkage mapping.
Methods S4 Calculating genetic correlations and broad-sense heritabilities.
Methods S5 Permutation test for cluster analysis.
Methods S6 Randomization test.
Methods S7 Quantifying QTL overlap and permutation test.
Methods S8 Predicting genetic correlations from QTL properties and permutation analysis.
Methods S9 Fraser v-test statistic.

Notes S1 Analyses using only genome-wide significant QTLs.
Notes S2 Ascertainment bias analysis and results.

Table S1 List of individuals phenotyped but NOT genotyped
Table S2 Broad-sense heritabilities for the 13 phenotypic traits measures.
Table S3 Genetic correlations derived from variance-covariance components for the 13 phenotypic traits measured.
Table S4 QTL characteristics for all trait QTLs.
Table S5 Summary of aggregate QTL characteristics for individual traits
Table S6 Pairwise QTL overlap.
Table S7 Average predicted genetic correlations, r_Q, within and between modules with standard errors (in parentheses).
Table S8 Randomization test (random placement of QTLs in genome) of whether QTLs within modules are spatially clustered in the genome.
Table S9 Genetic variances and covariances for the 13 phenotypic traits measured
Table S10 Number of QTLs with effects in same direction as or opposite direction from difference between species.
Table S11 Contra-directional QTLs summary.
Table S12 Directionality of QTLs that overlap for each pair of traits.
Table S13 Divergence correlations between nectar and floral traits from studies of pollination syndromes.

REFERENCES

Anderson EC, Slatkin M. **2003**. Orr's quantitative trait loci sign test under conditions of trait ascertainment. *Genetics* **165**: 445–446.

Armbruster WS, Pélabon C, Bolstad GH, Hansen TF. **2014**. Integrated phenotypes: Understanding trait covariation in plants and animals. *Philosophical Transactions of the Royal Society B: Biological Sciences* **369**: 1–16.

Armbruster WS, Pelabon C, Hensen TF, Mulder CPH. **2004**. Floral integration, Modularity, and Accuracy: Distinguishing Complex Adaptations from Genetic Constraints. In: Pigliuci M, Preston K, eds. Phenotypic Integration: Studying the Ecology and Evolution of Complex Phenotypes. New York, NY, USA: Oxford University Press, 22–49.

Armbruster WS, Di Stilio VS, Tuxill JD, Flores TC, Runk JLV. **1999**. Covariance and Decoupling of Floral and Vegetative Traits in Nine Neotropical Plants: A Re-Evaluation of Berg's Correlation-Pleiades Concept. *American Journal of Botany* **86**: 39–55.

Arnold SJ. **1992**. Constraints on Phenotypic Evolution. *The American Naturalist* **140**: S85–S107.

Arnold SJ, Bürger R, Hohenlohe PA, Ajie BC, Jones AG. **2008**. Understanding the evolution and stability of the G-matrix. *Evolution* **62**: 2451–2461.

Arunkumar R, Ness RW, Wright SI, Barrett SCH. **2015**. The Evolution of Selfing Is Accompanied by Reduced Efficacy of Selection and Purging of Deleterious Mutations. *Genetics* **199**: 817–829.

Ashman T-L, Majetic CJ. **2006**. Genetic constraints on floral evolution: a review and evaluation of patterns. *Heredity* **96**: 343–352.

Baker HG, Baker I. **1983**. Floral nectar sugar constituents in relation to pollinator type. In: Jones CE, Little RJ, eds. Handbook of Pollination Biology. New York, NY, USA: Van Nostrand Reinhold, 117–141.

Baker HG, Baker I. **1990**. The predictive value of nectar chemistry to the recognition of pollinator types. *Israel Journal of Botany* **39**: 157–166.

Baldwin BG, Kalisz S, Armbruster WS. **2011**. Phylogenetic perspectives on diversification, biogeography, and floral evolution of Collinsia and Tonella (Plantaginaceae). *American Journal of Botany* **98**: 731–753.

Barrett SCH. **2002**. The Evolution of Plant Sexual Diversity. *Nature Reviews Genetics* **3**: 274–284.

Baum SF, Eshed Y, Bowman JL. **2001**. The *Arabidopsis* nectary is an ABC-independent floral structure. *Development* **128**: 4657–67.

Beavis WD, Smith OS, Grant D, Fincher R. **1994**. Identification of quantitative trait loci using a small sample of topcrossed and F4 progeny from maize. *Crop Science* **34**: 882–896.

Benjamini Y, Hochberg Y. **1995**. Controlling the False Discovery Rate : A Practical and Powerful Approach to

Multiple Testing. *Journal of the Royal Statistical Society. Series B (Methodological)* **57**: 289–300.

Berg RL. **1960**. The Ecological Significance of Correlation Pleiades. *Evolution* **14**: 171–180.

Bowman JL, Smyth DR, Meyerowitz EM. **1989**. Genes directing flower development in *Arabidopsis*. *The Plant Cell* **1**: 37–52.

Brandon RN. **1999**. The Units of Selection Revisited: The Modules of Selection. *Biology and Philosophy* **14**: 167–180.

Broman KW, Gatti DM, Simecek P, Furlotte NA, Prins P, Sen Ś, Yandell BS, Churchill GA. **2019**. R/qtl2: Software for mapping quantitative trait loci with high-dimensional data and multiparent populations. *Genetics* **211**: 495–502.

Broman KW, Wu H, Sen S, Churchill GA. **2003**. R/qtl: QTL mapping in experimental crosses. *Bioinformatics* **19**: 889–890.

Bruneau A. **1997**. Evolution and homology of bird pollination syndromes in *Erythrina* (Leguminosae). *American Journal of Botany* **84**: 54–71.

Chen D, Yan W, Fu LY, Kaufmann K. **2018**. Architecture of gene regulatory networks controlling flower development in *Arabidopsis thaliana*. *Nature Communications* **9**: 1–13.

Cheverud JM. **1984**. Quantitative genetics and developmental constraints on evolution by selection. *Journal of Theoretical Biology* **110**: 155–171.

Coen ES, Meyerowitz EM. **1991**. The war of the whorls: genetic interactions controlling flower development. *Nature* **353**: 31–37.

Conner JK, Cooper IA, La Rosa RJ, Pérez SG, Royer AM. **2014**. Patterns of phenotypic correlations among morphological traits across plants and animals. *Philosophical Transactions of the Royal Society B: Biological Sciences* **369**: 20130246.

Cronk Q, Ojeda I. **2008**. Bird-pollinated flowers in an evolutionary and molecular context. *Journal of Experimental Botany* **59**: 715–727.

von Dassow G, Munro E. **1999**. Modularity in Animal Development and Evolution: Elements of a Conceptual Framework for EvoDevo. *Journal of Experimental Zoology (Molecular and Developmental Evolution)* **325**: 1–19.

Dellinger AS. **2020**. Pollination syndromes in the 21st century: where do we stand and where may we go? *New Phytologist* **228**: 1193–1213.

Dellinger AS, Artuso S, Pamperl S, Michelangeli FA, Penneys DS, Fernández-Fernández DM, Alvear M, Almeda F, Scott Armbruster W, Staedler Y, *et al.* 2019. Modularity increases rate of floral evolution and adaptive success for functionally specialized pollination systems. *Communications Biology* **2**: 453.

Diggle PK. **2014**. Modularity and intra-floral integration in metameric organisms: plants are more than the sum of their parts. *Philosophical Transactions of the Royal Society B: Biological Sciences* **369**: 20130253.

Duncan TM, Rausher MD. **2013a**. Morphological and genetic differentiation and reproductive isolation among

closely related taxa in the *Ipomoea* series *Batatas*. *American Journal of Botany* **100**: 2183–2193.

Duncan TM, Rausher MD. **2013b**. Evolution of the selfing syndrome in *Ipomoea*. *Frontiers in Plant Science* **4**: 301.

Dupont YL, Hansen DM, Rasmussen JT, Olesen JM. **2004**. Evolutionary changes in nectar sugar composition associated with switches between bird and insect pollination: The Canarian bird-flower element revisited. *Functional Ecology* **18**: 670–676.

Edwards MB, Choi GPT, Derieg NJ, Min Y, Diana AC, Hodges SA, Mahadevan L, Kramer EM, Ballerini ES. **2021**. Genetic architecture of floral traits in bee- and hummingbird-pollinated sister species of *Aquilegia* (columbine). *Evolution* **75**: 2197–2216.

Falconer DS, Mackay TFC. **1996**. *Introduction to quantitative genetics*. Essex, UK: Longman Group Ltd.

Fenster CB, Ritland K. **1994**. Quantitative genetics of mating system divergence in the yellow monkeyflower species complex. *Heredity* **73**: 422–435.

Fishman L, Beardsley PM, Stathos A, Williams CF, Hill JP. **2015**. The genetic architecture of traits associated with the evolution of self-pollination in *Mimulus*. *New Phytologist* **205**: 907–917.

Fishman L, Kelly AJ, Willis JH. **2002**. Minor Quantitative Trait Loci Underlie Floral Traits Associated with Mating System Divergence in *Mimulus*. *Evolution* **56**: 2138.

Frazee LJ, Rifkin J, Maheepala DC, Grant A-G, Wright S, Kalisz S, Litt A, Spigler R. **2021**. New genomic resources and comparative analyses reveal differences in floral gene expression in selfing and outcrossing *Collinsia* sister species. *G3 Genes|Genomes|Genetics* **11**: 10.1093/g3journal/jkab177.

Fujikura U, Jing R, Hanada A, Takebayashi Y, Sakakibara H, Yamaguchi S, Kappel C, Lenhard M. **2018**. Variation in Splicing Efficiency Underlies Morphological Evolution in *Capsella*. *Developmental Cell* **44**: 192-203.e5.

Galetto L, Bernardello G. **2004**. Floral nectaries, nectar production dynamics and chemical composition in six *Ipomoea* species (Convolvulaceae) in relation to pollinators. *Annals of Botany* **94**: 269–280.

Galliot C, Hoballah ME, Kuhlemeier C, Stuurman J. **2006**. Genetics of flower size and nectar volume in *Petunia* pollination syndromes. *Planta* **225**: 203–12.

Gardner KM, Latta RG. **2007**. Shared quantitative trait loci underlying the genetic correlation between continuous traits. *Molecular Ecology* **16**: 4195–4209.

Goodwillie C, Sargent RD, Eckert CG, Elle E, Geber MA, Johnston MO, Kalisz S, Moeller DA, Ree RH, Vallejo-Marin M, *et al.* 2010. Correlated evolution of mating system and floral display traits in flowering plants and its implications for the distribution of mating system variation. *New Phytologist* **185**: 311–321.

Jeiter J, Hilger HH, Smets EF, Weigend M. **2017**. The relationship between nectaries and floral architecture: A case study in Geraniaceae and Hypseocharitaceae. *Annals of Botany* **120**: 791–803.

Juenger T, Pérez-Pérez JM, Bernal S, Micol JL. **2005**. Quantitative trait loci mapping of floral and leaf morphology traits in *Arabidopsis thaliana*: evidence for modular genetic architecture. *Evolution & Development* **7**: 259–

271.

Kaczorowski RL, Gardener MC, Holtsford TP. **2005**. Nectar Traits in *Nicotiana* Section *Alatae* (Solanaceae) in Relation to Floral Traits, Pollinators, and Mating System. *American Journal of Botany* **92**: 1270–1283.

Kaczorowski RL, Juenger TE, Holtsford TP. **2008**. Heritability and correlation structure of nectar and floral morphology traits in *Nicotiana alata*. *Evolution* **62**: 1738–1750.

Katzer AM, Wessinger CA, Hileman LC. **2019**. Nectary size is a pollination syndrome trait in *Penstemon*. *New Phytologist* **223**: 377–384.

Klingenberg CP. **2008**. Morphological Integration and Developmental Modularity. *Annual Review of Ecology, Evolution, and Systematics* **39**: 115–132.

Kostyun JL, Gibson MJS, King CM, Moyle LC. **2019**. A simple genetic architecture and low constraint allow rapid floral evolution in a diverse and recently radiating plant genus. *New Phytologist* **223**: 1009–1022.

Lande R, Arnold SJ. **1983**. The Measurement of Selection on Correlated Characters. *Evolution* **37**: 1210–1226.

Lewis JJ, Van Belleghem SM. **2020**. Mechanisms of Change: A Population-Based Perspective on the Roles of Modularity and Pleiotropy in Diversification. *Frontiers in Ecology and Evolution* **8**: 1–8.

Lewontin RC. 1978. Adaptation. *Scientific American* **239**: 212–231.

McDonald JA, Hansen DR, McDill JR, Simpson BB. **2011**. A Phylogenetic Assessment of Breeding Systems and Floral Morphology of North American *Ipomoea* (Convolvulaceae). *Journal of the Botanical Research Institute of Texas* **5**: 159–177.

Melo D, Porto A, Cheverud JM, Marroig G. **2016**. Modularity: Genes, Development, and Evolution. *Annual Review of Ecology, Evolution, and Systematics* **47**: 463–486.

Milligan SB, Balzarini M, White WH. **2003**. Broad-sense heritabilities, genetic correlations, and selection indices for sugarcane borer resistance and their relation to yield loss. *Crop Science* **43**: 1729–1735.

Mitchell-Olds T, Rutledge J. J. 1986. Quantitative Genetics in Natural Plant Populations: A Review of the Theory. *The American Naturalist* **127**: 379–402.

Müllner D. **2013**. Fastcluster: Fast hierarchical, agglomerative clustering routines for R and Python. *Journal of Statistical Software* **53**: 1–18.

Muñoz-Rodríguez P, Carruthers T, Wood JRI, Williams BRM, Weitemier K, Kronmiller B, Ellis D, Anglin NL, Longway L, Harris SA, *et al.* 2018. Reconciling Conflicting Phylogenies in the Origin of Sweet Potato and Dispersal to Polynesia. *Current Biology* **28**: 1246-1256.e12.

Nakazato T, Rieseberg LH, Wood TE. **2013**. The genetic basis of speciation in the *Giliopsis* lineage of *Ipomopsis* (Polemoniaceae). *Heredity* **111**: 227–237.

Ordano M, Fornoni J, Boege K, Domínguez CA. **2008**. The adaptive value of phenotypic floral integration. *New Phytologist* **179**: 1183–1192.

Orr HA. **1998**. Testing natural selection vs. genetic drift in phenotypic evolution using quantitative trait locus data. *Genetics* **149**: 2099–2104.

Ostevik KL. 2016. *The ecology and genetics of adaptation and speciation in dune sunflowers*. PhD thesis, University of British Columbia, Vancouver, BC, Canada.

Parachnowitsch AL, Manson JS, Sletvold N. **2019**. Evolutionary ecology of nectar. *Annals of Botany* **123**: 247–261.

Pelaz S, Ditta GS, Baumann E, Wisman E, Yanofsky MF. **2000**. B and C floral organ identity functions require *SEPALLATA* MADS-box genes. *Nature* **405**: 200–203.

Peterson BK, Weber JN, Kay EH, Fisher HS, Hoekstra HE. **2012**. Double Digest RADseq: An Inexpensive Method for De Novo SNP Discovery and Genotyping in Model and Non-Model Species. *PLoS ONE* **7**: e37135.

R Core Team. R: A language and environment for statistical computing. https://www.R-project.org.

Rastas P. **2017**. Lep-MAP3: Robust linkage mapping even for low-coverage whole genome sequencing data. *Bioinformatics* **33**: 3726–3732.

Reich D, Berger A, von Balthazar M, Chartier M, Sherafati M, Schönenberger J, Manafzadeh S, Staedler YM. **2020**. Modularity and evolution of flower shape: the role of function, development, and spandrels in *Erica*. *New Phytologist* **226**: 267–280.

Rifkin JL, Cao G, Rausher MD. **2021**. Genetic architecture of divergence: the selfing syndrome in *Ipomoea lacunosa*. *American Journal of Botany* **108**: 2038–2054.

Rifkin JL, Castillo AS, Liao IT, Rausher MD. **2019a**. Gene flow, divergent selection and resistance to introgression in two species of morning glories (*Ipomoea*). *Molecular Ecology* **28**: 1709–1729.

Rifkin JL, Liao IT, Castillo AS, Rausher MD. **2019b**. Multiple aspects of the selfing syndrome of the morning glory *Ipomoea lacunosa* evolved in response to selection: A Qst-Fst comparison. *Ecology and Evolution* **9**: 7712–7725.

Roff DA. **2007**. A centennial celebration for quantitative genetics. *Evolution* **61**: 1017–1032.

Sas C, Müller F, Kappel C, Kent T V, Wright SI, Hilker M, Lenhard M. **2016**. Repeated Inactivation of the First Committed Enzyme Underlies the Loss of Benzaldehyde Emission after the Selfing Transition in Capsella. *Current Biology* **26**: 3313–3319.

Sedlazeck FJ, Rescheneder P, Von Haeseler A. **2013**. NextGenMap: Fast and accurate read mapping in highly polymorphic genomes. *Bioinformatics* **29**: 2790–2791.

Sheridan A, Barker J. **1974**. Two-trait Selection and the Genetic Correlation II. Changes in the Genetic Correlation During Two-trait Selection. *Australian Journal of Biological Sciences* **27**: 89.

Slavković F, Dogimont C, Morin H, Boualem A, Bendahmane A. **2021**. The Genetic Control of Nectary Development. *Trends in Plant Science* **26**: 260–271.

Slotte T, Hazzouri KM, Stern D, Andolfatto P, Wright SI. **2012**. Genetic Architecture and Adaptive

Significance of the Selfing Syndrome in *Capsella*. *Evolution* **66**: 1360–1374.

Smith SD. **2016**. Pleiotropy and the evolution of floral integration. *New Phytologist* **209**: 80–85.

Smyth DR, Bowman JL, Meyerowitz EM. **1990**. Early flower development in *Arabidopsis*. *The Plant Cell* **2**: 755–767.

Strandh M, Jönsson J, Madjidian JA, Hansson B, Lankinen Å. **2017**. Natural selection acts on floral traits associated with selfing rate among populations of mixed-mating *Collinsia heterophylla* (Plantaginaceae). *International Journal of Plant Sciences* **178**: 594–606.

Stuurman J, Hoballah ME, Broger L, Moore J, Basten C, Kuhlemeier C. **2004**. Dissection of floral pollination syndromes in *Petunia*. *Genetics* **168**: 1585–1599.

Tavares DC, Freitas L, Gaglianone MC. **2016**. Nectar volume is positively correlated with flower size in hummingbird-visited flowers in the Brazilian Atlantic Forest. *Journal of Tropical Ecology* **32**: 335–339.

Thornburg RW. **2007**. Molecular biology of the *Nicotiana* floral nectary. In: Nicolson SW, Nepi M, Pacini M, eds. Nectaries and Nectar. Dordrecht, The Netherlands: Springer, 265–288.

USDA, NRCS. **2021**. The PLANTS Database (http://plants.sc.egov.usda.gov, 06/03/2021). National Plant Data Team, Greensboro, NC USA.

Verd B, Monk NAM, Jaeger J. **2019**. Modularity, criticality, and evolvability of a developmental gene regulatory network. *eLife* **8**: 1–40.

Wagner GP, Altenberg L. **1996**. Complex Adaptations and the Evolution of Evolvability. *Evolution* **50**: 967–976.

Wagner GP, Pavlicev M, Cheverud JM. **2007**. The road to modularity. *Nature Reviews Genetics* **8**: 921–931.

Wessinger CA, Hileman LC. **2016**. Accessibility, constraint, and repetition in adaptive floral evolution. *Developmental Biology* **419**: 175–183.

Wessinger CA, Hileman LC, Rausher MD. **2014**. Identification of major quantitative trait loci underlying floral pollination syndrome divergence in *Penstemon*. *Philosophical Transactions of the Royal Society B: Biological Sciences* **369**: 20130349–20130349.

Worley AC, Barrett SCH. **2000**. Evolution of Floral Display in *Eichhornia paniculata* (Pontederiaceae): Direct and Correlated Responses to Selection on Flower Size and Number. *Evolution* **54**: 1533–1545.

Wozniak NJ, Kappel C, Marona C, Altschmied L, Neuffer B, Sicard A. **2020**. A Similar Genetic Architecture Underlies the Convergent Evolution of the Selfing Syndrome in *Capsella*. *The Plant Cell*: tpc.00551.2019.

Xu S. **2003**. Theoretical Basis of the Beavis Effect. *Genetics* **165**: 2259–2268.

Yang J, Zaitlen NA, Goddard ME, Visscher PM, Price AL. **2014**. Advantages and pitfalls in the application of mixed-model association methods. *Nature Genetics* **46**: 100–106.

Fig. 1 Flowers and traits measured in the study

a) Images of the two sister morning glory species used in the study, *Ipomoea cordatotriloba* (left) and *I. lacunosa* (right). Scale bar = 1 cm. b) Floral size traits measured in the study. c) Image of the nectary (cream-colored tissue surrounding the ovary) with purple points as landmarks for estimating the nectary size. *Ipomoea cordatotriloba* (left) and *I. lacunosa* (right). Scale bar = 1 cm. d) Nectary size approximated as the volume of the outer frustrum minus the inner frustrum. Formula for calculating the nectary size is as follows: $V = \frac{\pi h}{3}\left[\left(r_1^2 + r_1 r_2 + r_2^2\right) - \left(r_3^2 + r_3 r_4 + r_4^2\right)\right]$, where h is the nectary height, r_1 is the nectary top outer radius, r_2 is the nectary top inner radius, r_3 is the nectary bottom outer radius, and r_4 is the nectary bottom inner radius.

Fig. 2 Cluster diagram and heatmap based on variance-covariance-component genetic correlations.

Cluster dendrogram portrayed for the "mcquitty" method. Boxes in the heatmap indicate the three clusters. Other clustering methods result in the same three clusters (Supporting Information Fig. S6). For the heatmap, strong positive correlations are in dark purple while weak to no correlation range from light purple to white. Cluster diagram on top from left to right: seed, nectar, and flower size. Pairwise genetic correlation values are found in Table S3.

Fig. 3 Chromosome map of QTLs for 13 phenotypic traits.

Each bar represents the 1.5 LOD confidence interval with the vertical line indicating the QTL peak. Bars in orange hues represent seed traits; maroon red hues represent nectar traits; purple hues represent floral size traits. A summary of QTL peaks is found in Supporting Information Table S4. Individual trait QTL plots are found in Fig. S7.

Fig. 4 Comparison between genetic correlations and QTL overlap.

Scatterplot of correlation between genetic correlations and QTL overlap (Supporting Information Table S6) for all trait pairs. Circles represent within-trait modules, and squares represent between-trait modules. Dark purple circles = floral size traits. Dark red circles = nectar traits. Orange circles = seed traits. Lavender squares = floral size and nectar traits. Peach squares = flower and seed traits. Dark orange-red squares = seed and nectar traits.

Fig. 5 Accuracy of predicted correlations.

The average total relative homozygous effect (RHE) was calculated by taking the average of total RHE for the two traits. Significance of correlation was determined by a permutation test. a) Correlation between r_G and predicted genetic correlations from QTL effects (r_Q) for all traits. b) Same as a) but excluding seed traits. c) Correlation between the average total RHE for all traits and the genetic correlation estimation bias (r_Q - r_G). d) Same as c) but excluding seed traits. For a) and c), orange points indicate correlations that include one of the seed traits; purple points indicate correlations of non-seed traits (floral size and nectar traits only).

The quantitative accuracy of the predicted genetic correlation is reflected in the bias, $r_Q - r_G$. Bias was significantly less for trait pairs with greater total RHE (Fig. 5c). Although this pattern holds after removing the correlations that include seed traits, the permutation test is not significant (Fig. 5d). For just nectar and floral size traits, average bias was -0.0968.

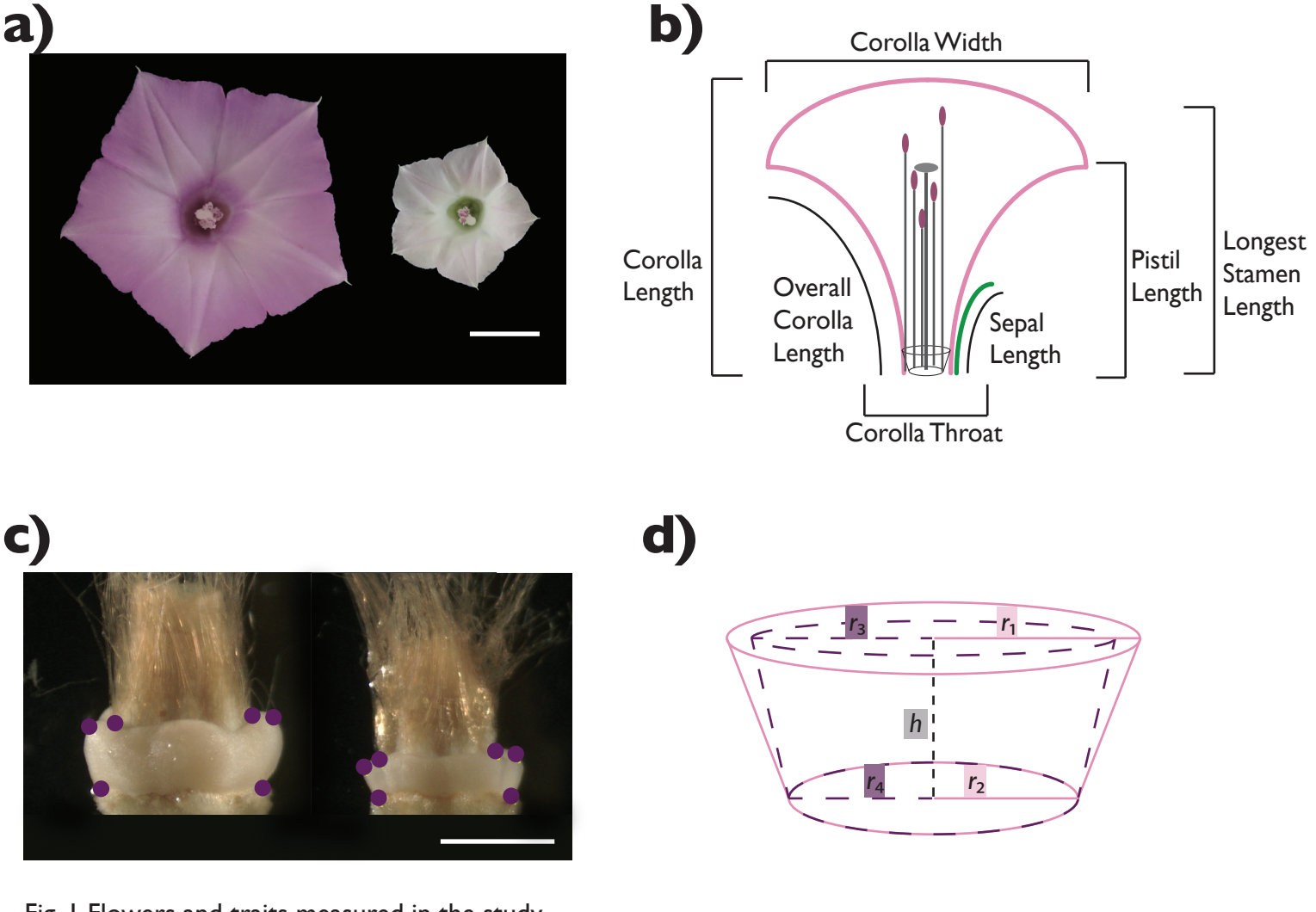

Fig. 1 Flowers and traits measured in the study

a) Images of the two sister morning glory species used in the study, *Ipomoea cordatotriloba* (left) and *I. lacunosa* (right). Scale bar = 1 cm. b) Floral size traits measured in the study. c) Image of the nectary (cream-colored tissue surrounding the ovary) with purple points as landmarks for estimating the nectary size. *Ipomoea cordatotriloba* (left) and *I. lacunosa* (right). Scale bar = 1 cm. d) Nectary size approximated as the volume of the outer frustrum minus the inner frustrum. Formula for calculating the nectary size is as follows: $V = \pi h/3\ [(r_1^2+r_1r_2+r_2^2)-(r_3^2+r_3r_4+r_4^2)]$, where h is the nectary height, r_1 is the nectary top outer radius, r_2 is the nectary top inner radius, r_3 is the nectary bottom outer radius, and r_4 is the nectary bottom inner radius.

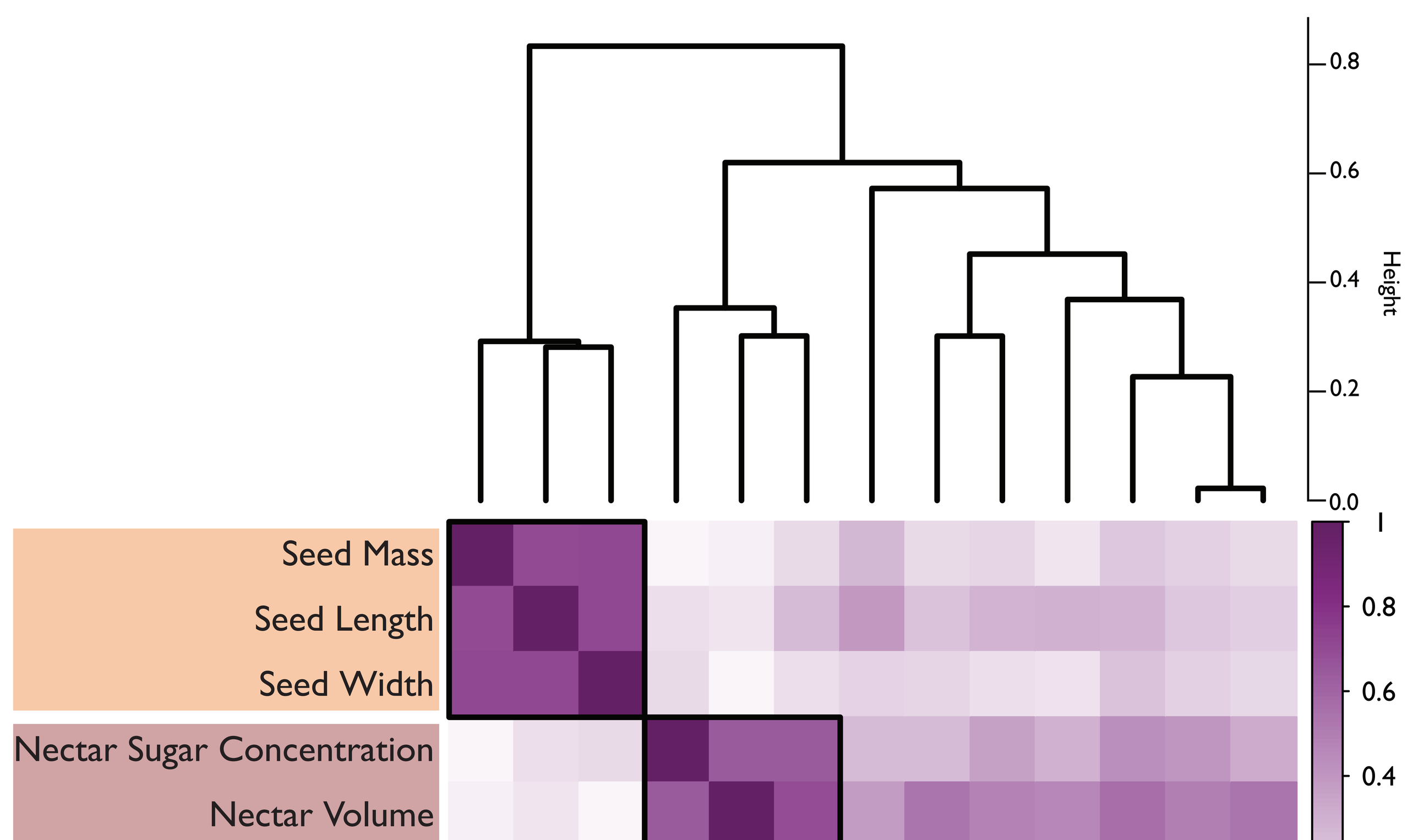

Fig. 2 Cluster diagram and heatmap based on variance-covariance-component genetic correlations. Cluster dendrogram portrayed for the "mcquitty" method. Boxes in the heatmap indicate the three clusters. Other clustering methods result in the same three clusters (Fig. S6). For the heatmap, strong positive correlations are in dark purple while weak to no correlation range from light purple to white. Cluster diagram on top from left to right: seed, nectar, and flower size. Pairwise genetic correlation values are found in Table S3.

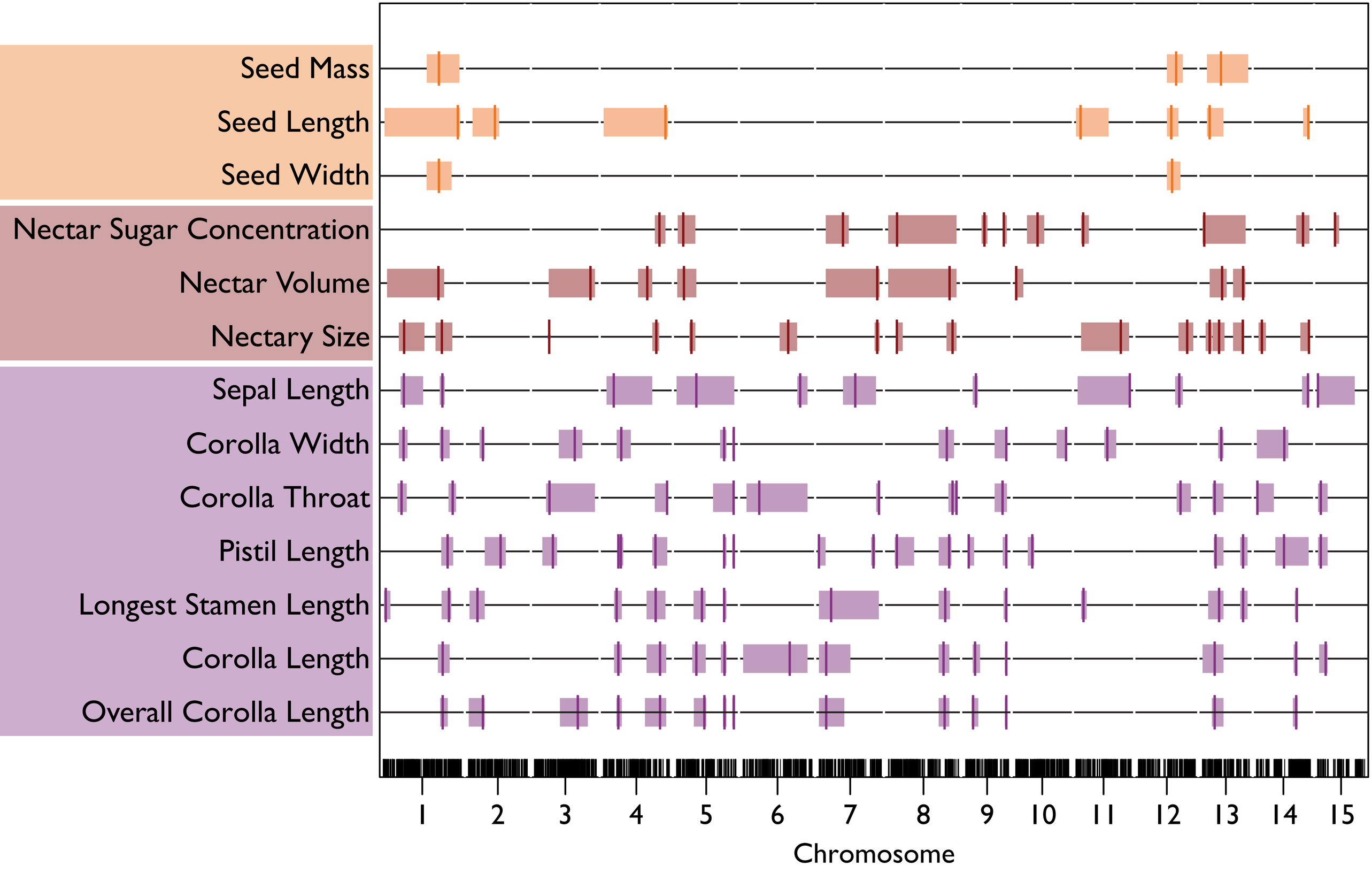

Fig. 3 Chromosome map of QTLs for 13 phenotypic traits.
Each bar represents the 1.5 LOD confidence interval with the vertical line indicating the QTL peak. Bars in orange hues represent seed traits; maroon red hues represent nectar traits; purple hues represent floral size traits. A summary of QTL peaks is found in Table S4. Individual trait QTL plots are found in Fig. S7.

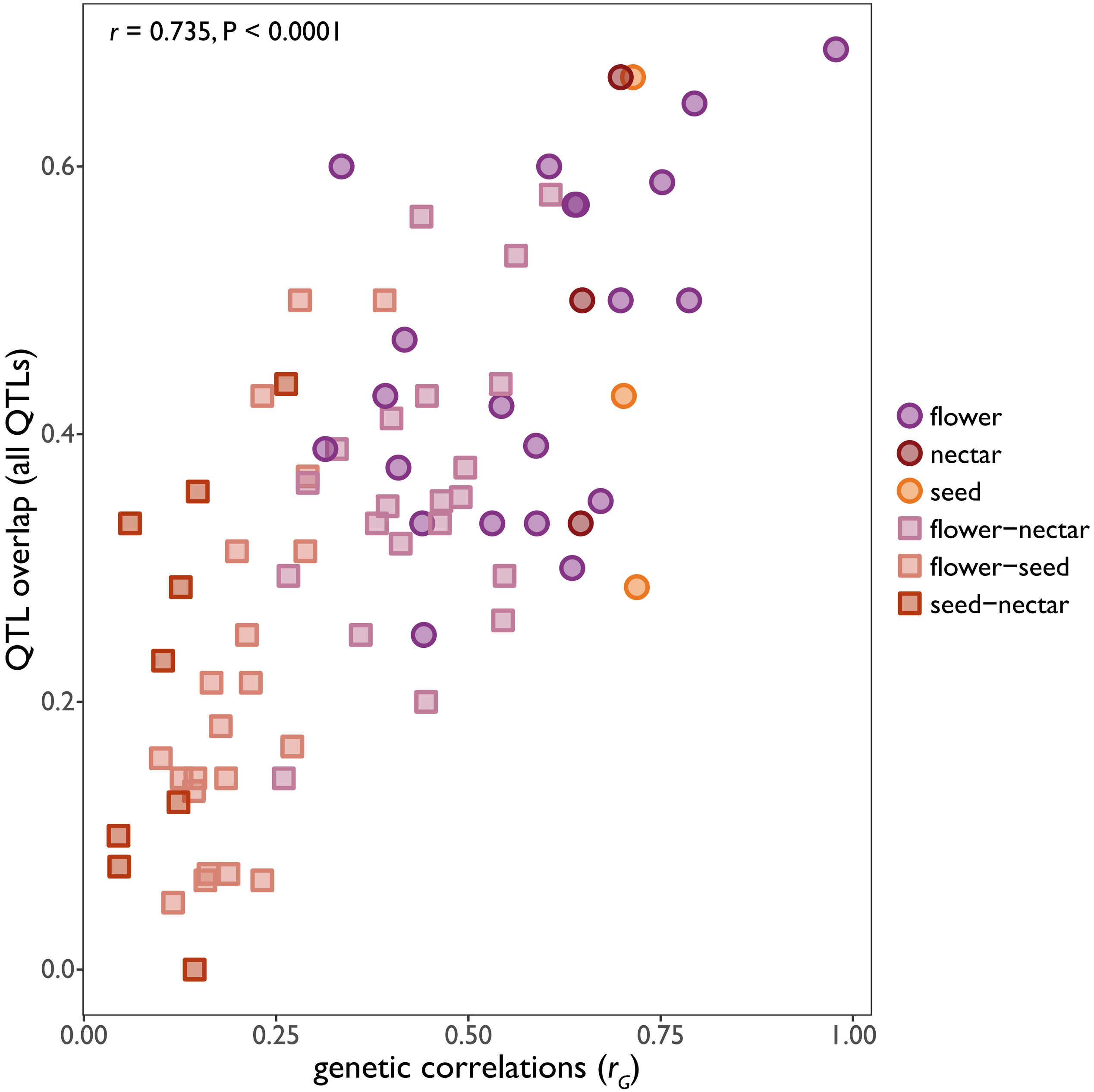

Fig. 4 Comparison between genetic correlations and QTL overlap.
Scatterplot of correlation between genetic correlations and QTL overlap (Table S6) for all trait pairs. Circles represent within-trait modules, and squares represent between-trait modules. Dark purple circles = floral size traits. Dark red circles = nectar traits. Orang¬¬e circles = seed traits. Lavender squares = floral size and nectar traits. Peach squares = flower and seed traits. Dark orange-red squares = seed and nectar traits.

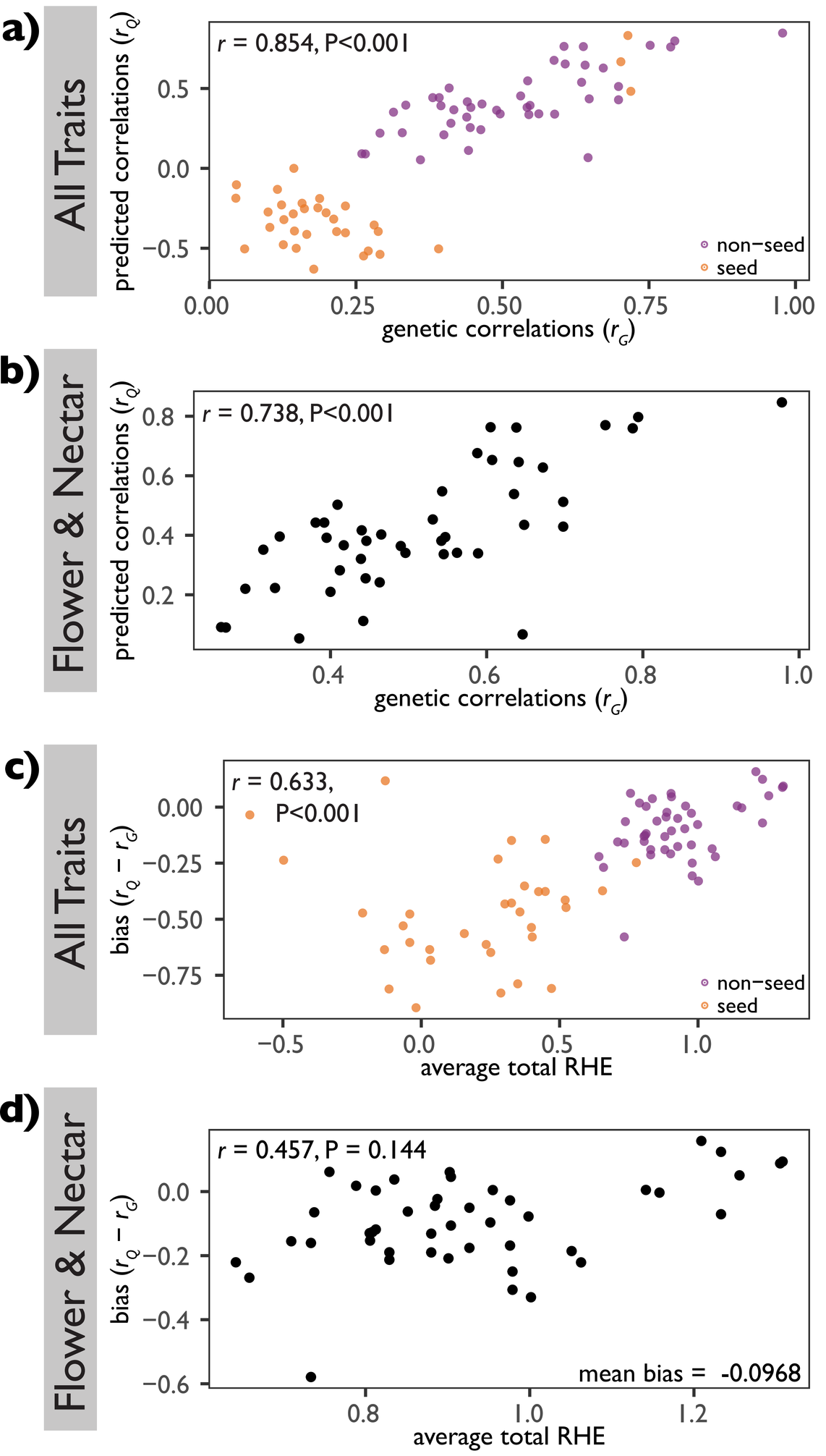

Fig. 5 Accuracy of predicted correlations.
The average total relative homozygous effect (RHE) was calculated by taking the average of total RHE for the two traits. Significance of correlation was determined by a permutation test. a) Correlation between r_G and predicted genetic correlations from QTL effects (r_Q) for all traits. b) Same as a) but excluding seed traits. c) Correlation between the average total RHE for all traits and the genetic correlation estimation bias (r_Q - r_G). d) Same as c) but excluding seed traits. For a) and c), orange points indicate correlations that include one of the seed traits; purple points indicate correlations of non-seed traits (floral size and nectar traits only).